

## Supplementary Material for 'Nuclear Quantum Effects on the Thermodynamic, Structural, and Dynamical Properties of Water'

Ali Eltareb<sup>1,3</sup>, Gustavo E. Lopez<sup>2,4</sup>, and Nicolas Giovambattista<sup>1,3,4</sup>

<sup>1</sup>Department of Physics, Brooklyn College of the City University of New York, Brooklyn, NY 11210, United States

<sup>2</sup>Department of Chemistry, Lehman College of the City University of New York, Bronx, NY 10468, United States

<sup>3</sup>Ph.D. Program in Physics, The Graduate Center of the City University of New York, New York, NY 10016

<sup>4</sup>Ph.D. Program in Chemistry, The Graduate Center of the City University of New York, New York, NY 10016

We provide additional results obtained from PIMD simulations of  $H_2O$  and  $D_2O$  using the q-TIP4P/F model. The main goal of this supplementary material is to show how sensitive the results in the main manuscript are to the (i) PIMD simulation time step  $dt$ , (ii) number of beads per polymer  $n_b$ , and (iii) collision frequency  $\gamma$  of the local PILE thermostat employed. The sensitivity of our results to  $dt$  is explored for both  $H_2O$  and  $D_2O$  for the cases  $dt = 0.1, 0.25, 0.50$  fs ( $H_2O$ ) and  $dt = 0.25, 0.50$  fs ( $D_2O$ ). The effects of varying  $n_b$  are also explored for both  $H_2O$  ( $n_b = 32, 72, 128$ ) and  $D_2O$  ( $n_b = 32, 72$ ). The effects of varying  $\gamma$  are studied only for the case of  $H_2O$  with  $\gamma = 1.0 - 10^{-6}$  ps<sup>-1</sup>; PIMD simulations for  $D_2O$  are all performed with  $\gamma = 0.001$  ps<sup>-1</sup>. The results for  $H_2O$  and  $D_2O$  included in the main manuscript correspond to  $dt = 0.25$  fs,  $n_b = 32, 72$ , and  $\gamma = 0.001$  ps<sup>-1</sup>.

### I. THERMODYNAMIC PROPERTIES

The densities of  $H_2O$  and  $D_2O$  as function of temperature are included in Fig. S1. Fig. S2 shows the enthalpy and isobaric heat capacity  $C_P(T)$  of  $H_2O$  and  $D_2O$ ; the corresponding isothermal compressibility  $\kappa_T(T)$  and dielectric constant  $\epsilon(T)$  are included in Figs. S3 and S4, respectively. The same symbol and color styles are employed in Figs. S1-S4 to denote the different system ( $H_2O$  and  $D_2O$ ) and conditions ( $dt$  and  $n_b$ ) considered.

The results can be summarized as follows. The reported  $\rho(T)$  (Fig. S1),  $\kappa_T(T)$  (Fig. S3), and  $\epsilon(T)$  (Fig. S4) of  $H_2O$  and  $D_2O$  are not sensitive, within error bars, to the values of  $n_b$  and  $dt$  explored (i.e.,  $dt = 0.10 - 0.50$  fs and  $n_b = 32 - 128$  for  $H_2O$ ;  $dt = 0.25 - 0.50$  fs and  $n_b = 32 - 72$  for  $D_2O$ ). However, the corresponding  $C_P(T)$  vary considerably (by 5 – 20 J/mol/K) depending on  $dt$ . Varying  $n_b$  in the range 32 – 128 also alters the heat capacity of  $H_2O$  and  $D_2O$ . Briefly, from the thermodynamic properties studied, only  $C_P$  and the enthalpy are sensitive to the computational details and hence, its determination requires further studies.

A maximum in  $C_P$  is not observable for any of the values of  $dt$  and  $n_b$  explored. Instead, we confirm that the maximum in  $\kappa_T(T)$  and  $\epsilon(T)$  reported in the main manuscript is independent of  $dt$  and  $n_b$ . All of these extrema in thermodynamic properties are consistent with the possibility that water exhibits a liquid-liquid critical point at low temperatures and positive pressures [1].

Indeed, these maxima in the reported thermodynamic response functions are usually observed in classical computer simulations of water and water-like models that exhibit a LLCP [2, 3].

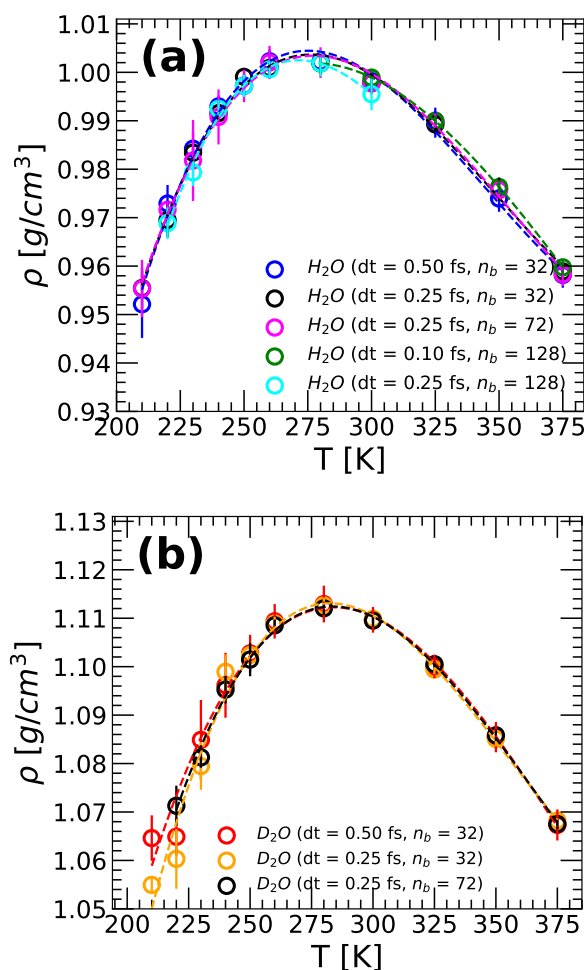


FIG. S1. Density of (a)  $H_2O$  and (b)  $D_2O$  as a function of temperature from PIMD simulations using the q-TIP4P/F model ( $P = 1$  bar). In both cases, PIMD simulations using different number of beads per ring-polymer  $n_b$  and time step  $dt$  give similar density values.

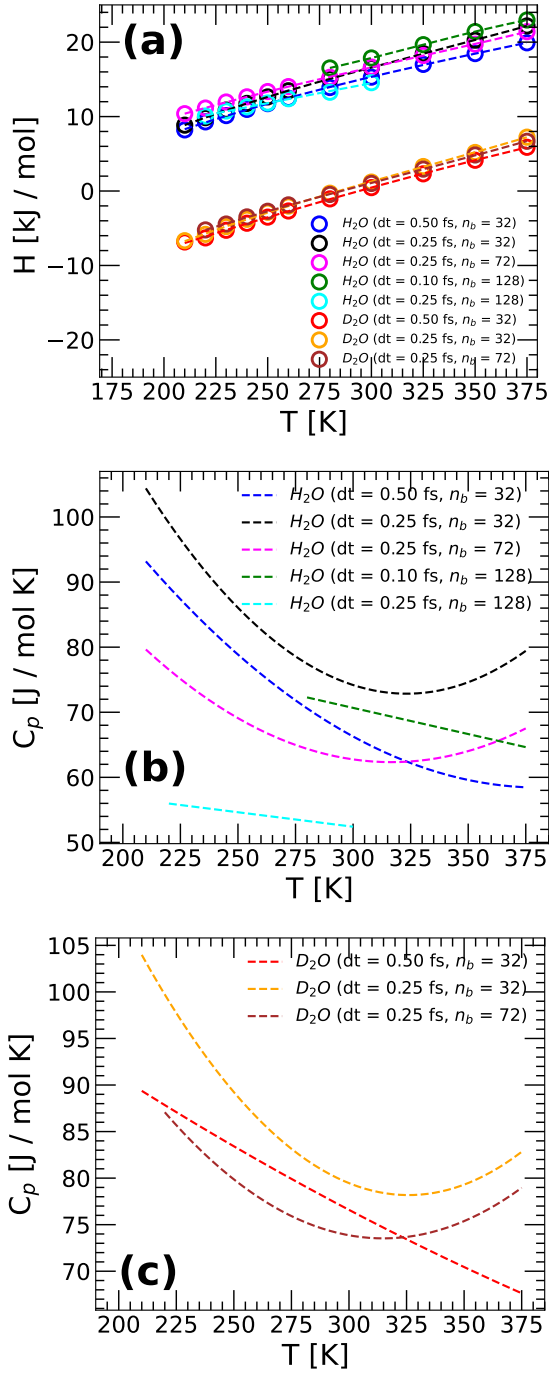


FIG. S2. (a) Enthalpy as a function of temperature for  $H_2O$  and  $D_2O$  ( $P = 1$  bar) obtained from PIMD simulations using the q-TIP4P/F model. Results are for different time steps  $dt$  and number of beads  $n_b$ . Lines are obtained using third-order polynomial fits of the PIMD simulation results. (b) Heat capacity  $C_P(T)$  of  $H_2O$  at different  $dt$  and  $n_b$  obtained from (a). (c)  $C_P(T)$  for  $D_2O$  calculated from (a).  $C_P(T)$  is very sensitive to both  $n_b$  and  $dt$ ; varying these parameters can lead to a change in  $C_P(T)$  of 5 - 50 J/mol/K and to the presence/absence of a minimum in  $C_P(T)$ .

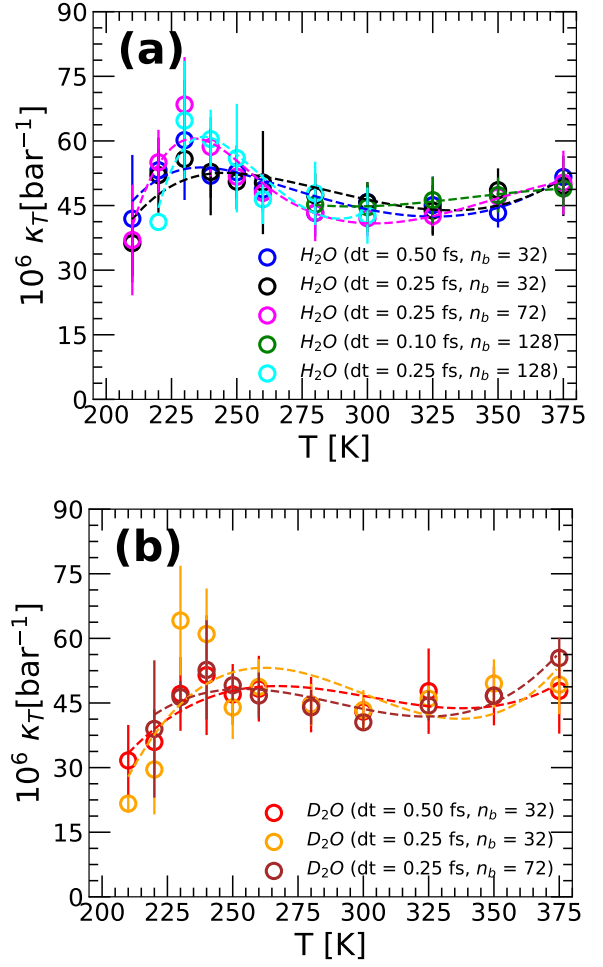


FIG. S3. Isothermal compressibility  $\kappa_T(T)$  as a function of temperature for (a)  $H_2O$  and (b)  $D_2O$  ( $P = 1$  bar). Results are from PIMD simulations using the q-TIP4P/F model and for different values of  $dt$  and  $n_b$ . The  $\kappa_T$  of both  $H_2O$  and  $D_2O$  are independent of the  $dt$  and  $n_b$  (within error bars).

## II. DYNAMICAL PROPERTIES

The diffusion coefficient of  $H_2O$  and  $D_2O$  as a function of temperature are included in Fig. S5; the reported diffusion coefficients are practically independent of the time step employed ( $dt = 0.10, 0.25, 0.50$  fs). The associated MSDs are included in Fig. S6a and S6b. As shown in Fig. S6c, the MSD, and hence the diffusion coefficients, are relatively independent of the number of beads  $n_b$  used. Fig. S7 shows the effects of the collision frequency  $\gamma$  on the  $MSD$  of  $H_2O$  for temperatures  $T = 220, 240,$  and  $300$  K. Hence, the diffusion coefficients obtained by using Eq. 8 in the main text are not affected by the thermostat used in the PIMD simulations.

We conclude by discussing briefly the methodology used in this work to calculate  $D(T)$ . In the RPMD technique, the diffusion coefficient is calculated from the Kubo-transformed velocity autocorrelation function

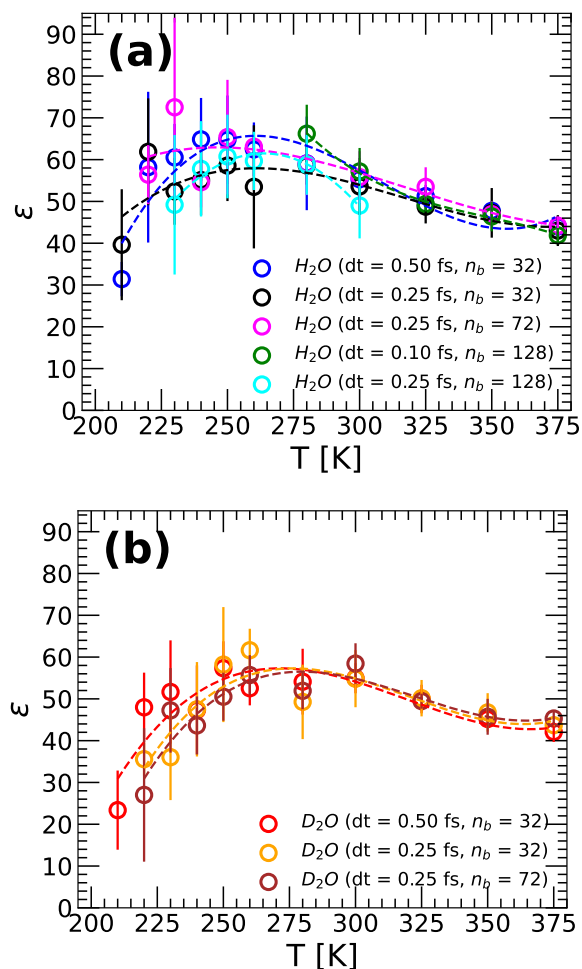


FIG. S4. Dielectric constant  $\epsilon(T)$  as a function of temperature of (a)  $H_2O$  and (b)  $D_2O$  ( $P = 1$  bar). Results are from PIMD simulations using the q-TIP4P/F model and for different values of  $dt$  and  $n_b$ . The  $\epsilon(T)$  of both  $H_2O$  and  $D_2O$  are independent of  $dt$  and  $n_b$  (within error bars).

(VACF); see manuscript, Eqs. 6 and 7. Moreover, the Kubo-transformed VACF is obtained from independent PIMD simulations at constant  $(N, V, E)$ . In Fig. S8, we include the values of  $D(T)$  calculated from RPMD. Specifically, we perform multiple PIMD simulations of  $H_2O$  in the NVE ensemble starting from configurations thermalized at  $T = 240, 280, 300, 325, 350, 375$  K. From these NVE trajectories, we calculate the Kubo-transformed VACF, from which  $D(T)$  is obtained (see Eq. 7 in the manuscript). At a given  $T$ ,  $\tilde{c}_{v-v}(t)$  is calculated from 10 independent trajectories (NVE ensemble) that vary in length depending on the temperature of the starting configuration. At  $T > 300$  K, 75-ps trajectories were used; for  $T = 300$  K and  $T < 300$  K, trajectories of 100 and 150 ps were used, respectively. As shown in Fig. S8, the values of  $D(T)$  reported in the main manuscript are identical (within error bars) to the values obtained using (true) RPMD.

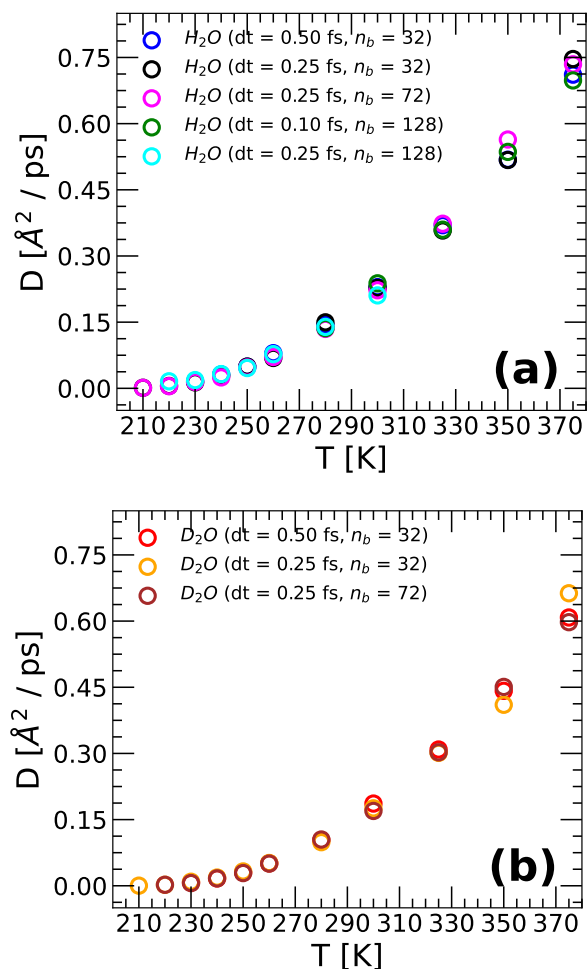


FIG. S5. Diffusion coefficient for (a)  $H_2O$  and (b)  $D_2O$  ( $P = 1$  bar) obtained from PIMD simulations using the q-TIP4P/F model. Results are for different time steps  $dt$  and number of beads  $n_b$ . The diffusion coefficients of both  $H_2O$  and  $D_2O$  are independent of  $dt$  and  $n_b$  (within error bars) at  $T < 350$  K.

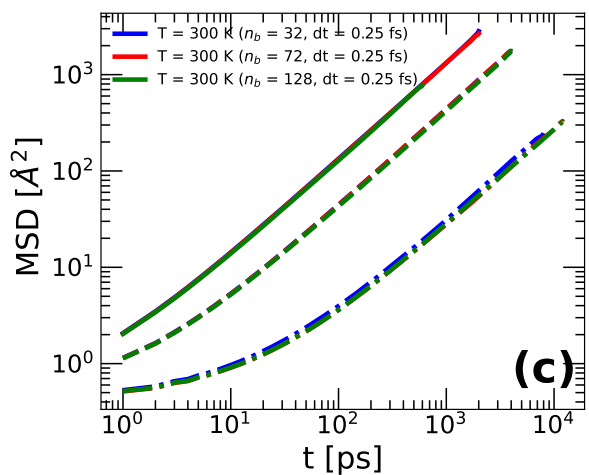
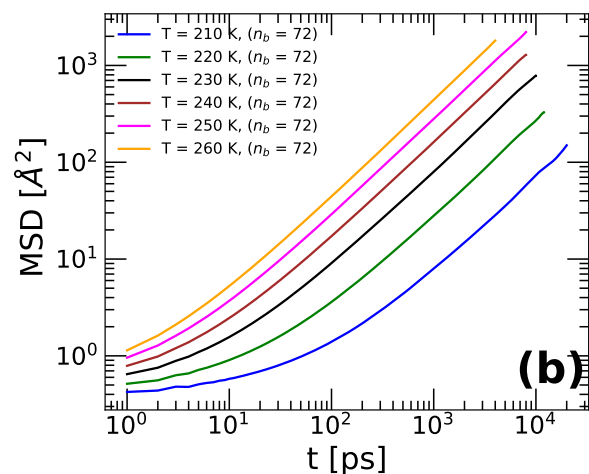
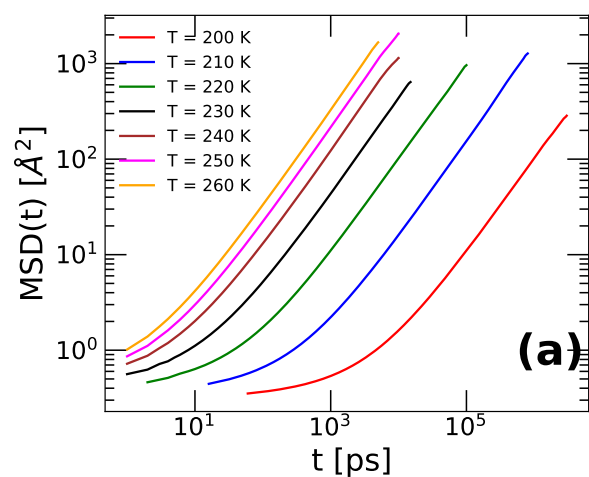


FIG. S6. MSD of water molecules from (a) classical MD and (b) PIMD simulations of q-TIP4P/F water ( $dt = 0.25$  fs;  $n_b = 72$ ). (c) Results from PIMD simulations are not sensitive to the number of beads  $n_b$  employed. Solid, dashed, and dot-dashed lines are, respectively, for  $T = 300$ ,  $260$ , and  $220$  K.

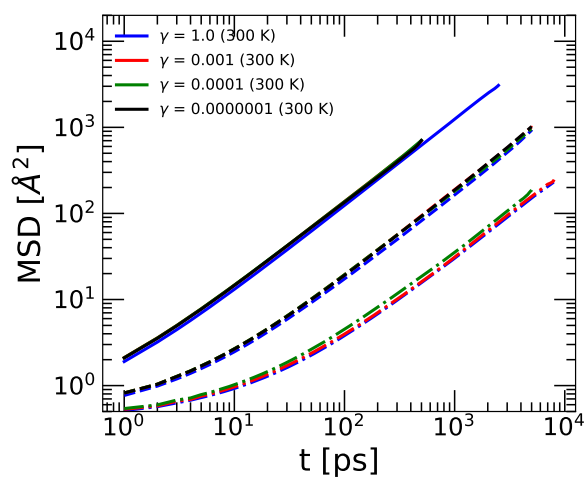


FIG. S7. Mean-square displacement of  $H_2O$  molecules obtained from PIMD simulations using the q-TIP4P/F model for different values of the thermostat collision frequency  $\gamma$  ( $dt = 0.50$  fs and  $n_b = 32$ ). Dashed and dotted lines correspond to  $T = 240$  K and  $T = 220$  K, respectively. The effects of  $\gamma$  on the dynamics of the system are negligible.

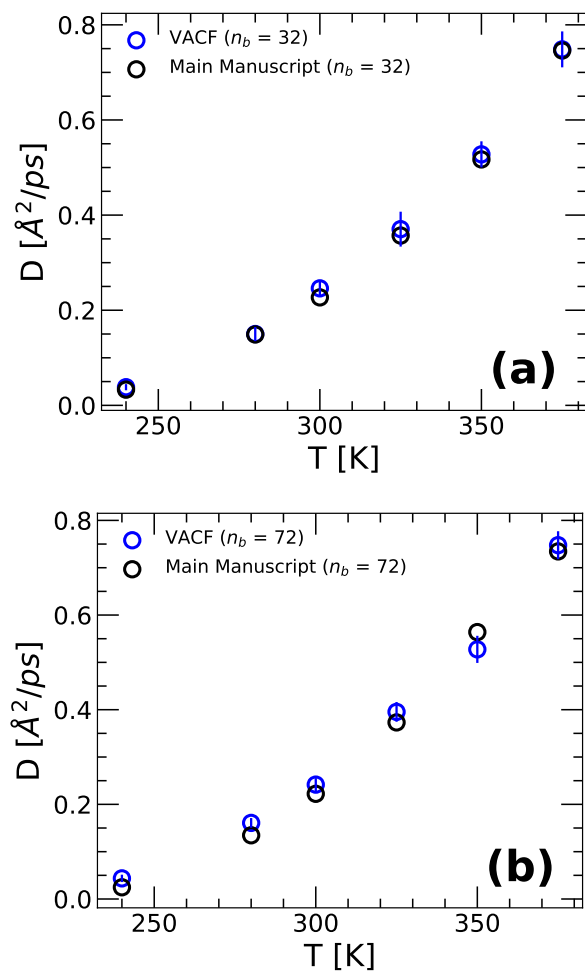


FIG. S8. (a) Diffusion coefficient of  $\text{H}_2\text{O}$  obtained from the Kubo-transformed velocity autocorrelation function  $\tilde{c}_{v.v}(t)$  (blue circles) and from the slope of the  $MSD$  (black circles; Eq. 8 of the main manuscript)  $n_b = 32$ . (b) Same as (a) but for  $n_b = 72$ . Both methods provide practically the same results for  $D$  (within error bars) reported in the main manuscript.

- 
- [1] P. Gallo, K. Amann-Winkel, C. A. Angell, M. A. Anisimov, F. Caupin, C. Chakravarty, E. Lascaris, T. Loerting, A. Z. Panagiotopoulos, J. Russo, *et al.*, Chem. Rev. **116**, 7463 (2016).
- [2] N. Giovambattista, Adv. Chem. Phys **152**, 113 (2013).
- [3] J. L. Abascal and C. Vega, J. Chem. Phys. **133**, 234502 (2010).